Journal of Medicinal Chemistry

Article

pubs.acs.org/jmc

Discovery of Pyrroloaminopyrazoles as Novel PAK Inhibitors

Chuangxing Guo,* Indrawan McAlpine,* Junhu Zhang, Daniel D. Knighton, Susan Kephart, M. Catherine Johnson, Haitao Li, Djamal Bouzida, Anle Yang, Liming Dong, Joseph Marakovits, Jayashree Tikhe, Paul Richardson, Lisa C. Guo, Robert Kania, Martin P. Edwards, Eugenia Kraynov, James Christensen, Joseph Piraino, Joseph Lee, Eleanor Dagostino, Christine Del-Carmen, Ya-Li Deng, Tod Smeal, and Brion W. Murray

Pfizer Global Research and Development, 10770 Science Center Drive, San Diego, California 92121, United States

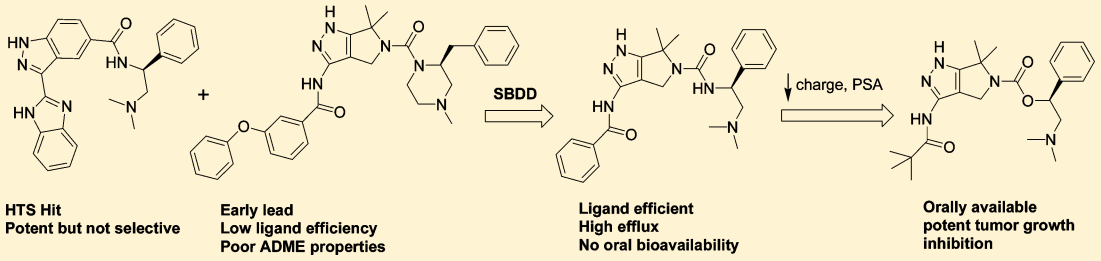

ABSTRACT: The P21-activated kinases (PAK) are emerging antitumor therapeutic targets. In this paper, we describe the discovery of potent PAK inhibitors guided by structure-based drug design. In addition, the efflux of the pyrrolopyrazole series was effectively reduced by applying multiple medicinal chemistry strategies, leading to a series of PAK inhibitors that are orally active in inhibiting tumor growth in vivo.

INTRODUCTION

The p21-activated kinase (PAK) family members are key effectors of Rho family GTPases, which act as regulatory switches that control such cellular processes as motility, proliferation, and cell survival.[1−5] The PAK family consists of PAK1,2,3 ("group A") and PAK4,5,6 ("group B"). A subset of the Rho GTPase family (such as Cdc42) have been shown to be required for Ras driven tumorigenesis.[3−5] PAK4 is a key effector for Cdc42 and mediates downstream signals that control cell motility, proliferation, and cell survival.[6−9] PAKs are known to regulate GTPases through phosphorylation of guanine nucleotide exchange factors (GEF). PAK1 and PAK4 directly phosphorylate GEF-H1 on Ser810.[10] Both PAK4 and PAK1 have been shown to be oncogenic and able to drive anchorage independent growth when activated.[11−13] PAK4 expression and activity are broadly up-regulated in solid tumors such as colon, ovarian, and pancreatic tumors. As such, inhibition of PAK4 presents a new opportunity for anticancer therapy.[14,15]

Our goal was to discover a potent, selective, orally active small-molecule PAK4 inhibitor. Multiple lead series were identified from a high throughput screening (HTS) campaign in which more than one million file compounds were tested for PAK4 enzymatic inhibition. A number of interesting screening hits were cocrystallized with the PAK4 kinase domain. Their cocrystal structures were solved, enabling structure-based drug design (SBDD) at the earliest stages of this program.

RESULTS AND DISCUSSION

Among the most potent hits from the PAK4 screening werer the benzimidazole-indole compounds, **1** and **2** (Figure 1). Knowledge from other internal kinase programs suggested that obtaining acceptable kinase selectivity would be challenging using this template. For a first-generation PAK4 inhibitor, we sought to avoid significant cross-activity with other kinases, especially those which might have toxicity concerns (e.g., LCK) or which might have mechanisms that would confound analysis (e.g., CDK2).

Another series, the pyrrolopyrazoles, originated from kinase counter-screenings from two other kinase programs, Aur2 and CDK2 (e.g., compound **3**, Figure 1). Compound **3** is active in both enzymatic and cellular assays and had encouraging selectivity for PAK4 in kinase counter-screening. As seen from the cocrystal of compound **3** in the PAK4 kinase domain (in Figure 2), the aminopyrazole forms the classic donor−acceptor−donor H-bond interactions with the PAK4 hinge region. The geminal dimethyl groups on the pyrrolopyrazole core pack well with Val-A335 and Met-A395 at the bottom of the binding pocket. The urea carbonyl oxygen makes a critical hydrogen bond with a conserved water molecule, which also solvates neighboring charged residues (Lys-A350 and Asp-A458) through hydrogen bond interactions. The basic nitrogen of the piperazine forms a charge−charge interaction with Asp-A458. The benzyl group coming off the piperazine fits well under the active site glycine loop. This crystal structure, along

Received: February 15, 2012

   dx.doi.org/10.1021/jm300204j | *J. Med. Chem.* XXXX, XXX, XXX−XXX

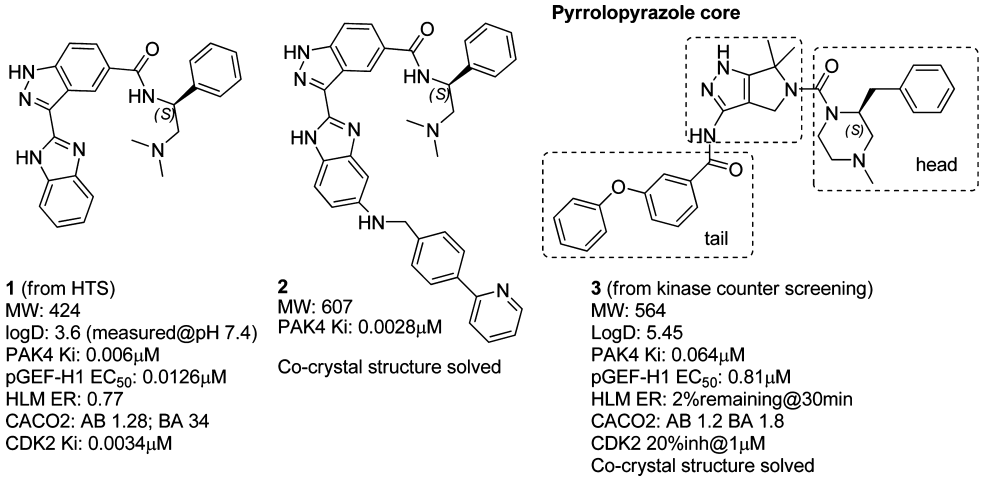

Figure 1. PAK4 leads.

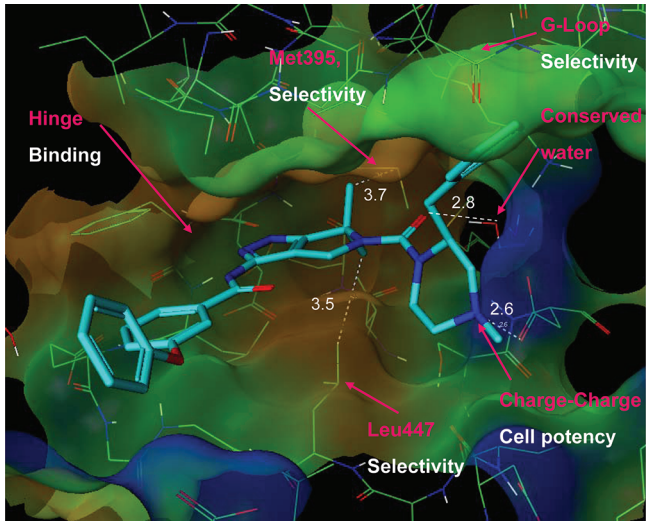

Figure 2. Co-crystal structure of compound **3** and PAK4KD (PDB code: 4APP) revealed key interactions.

with SAR on existing pyrazoles (data not shown), suggests the aminopyrazole is essential for potency, whereas the geminal dimethyl groups and the benzyl group are critical for kinase selectivity. The ligand−protein interactions involving the geminal dimethyl groups and the basic amine are also beneficial for potency, especially cellular activity.

The pyrrolopyrazole series generally has low ligand efficiency (LE < 0.3).[16] For example, compound **3** has a MW of 564, a measured log *D* of 5.45,[17] and is only moderately active in the enzymatic assay (K_i = 64 nM), which results in a LE = 0.14. Cellular activity was also modest (pGEF-H1 EC_{50} = 810 nM). At this point, poor metabolic stability and modest cell potency were the major issues for this series. From the legacy kinase programs, hundreds of close-in analogues were available for testing. The main strategy from previous programs was to lower lipophilicity by appending polar groups in tail region, often leading to analogues with even higher molecular weight (MW > 550). In this series, no compound with a better ADME profile was identified from this approach. Moreover, for a PAK4 inhibitor, cell potency (GEF-H1 EC_{50}) better than ∼200 nM could not be achieved using this tactic. The low ligand efficiency is likely the root cause of the observed poor metabolic stability and the flat cellular SAR for this series.

Our initial design strategy was to improve ligand efficiency by decreasing the size of the inhibitor while maintaining potency. Because the benzimidazole-indazole compound **1** is a more efficient ligand, the bound conformation of **3** was compared with that of **1** to define structural elements that are essential for binding. (Figure 3) The bound conformation of **1** was modeled from a cocrystal structure of its close analogue (**2**), which has an additional substituent on C-5 of the benzimidazole of **1**. This substituent is mostly solvent-exposed in its cocrystal structure with PAK4 so that its absence (as in **1**) would not significantly affect the bound conformation of the remaining

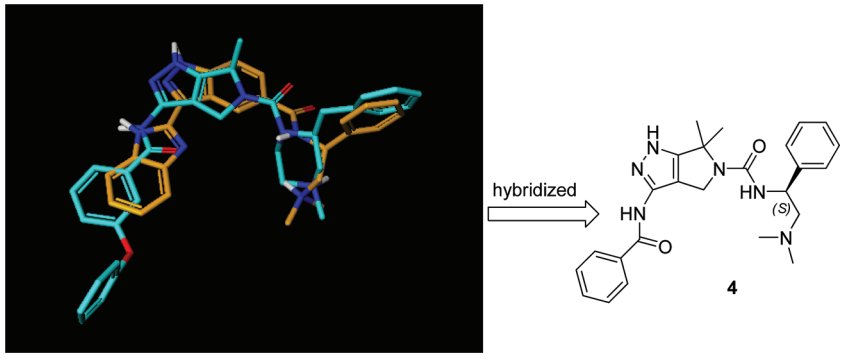

Figure 3. Bound conformation comparison: **3** (cocrystal) vs **1** (modeled).

dx.doi.org/10.1021/jm300204j | J. Med. Chem. XXXX, XXX, XXX−XXX

Scheme 1. Synthesis of Compound 4

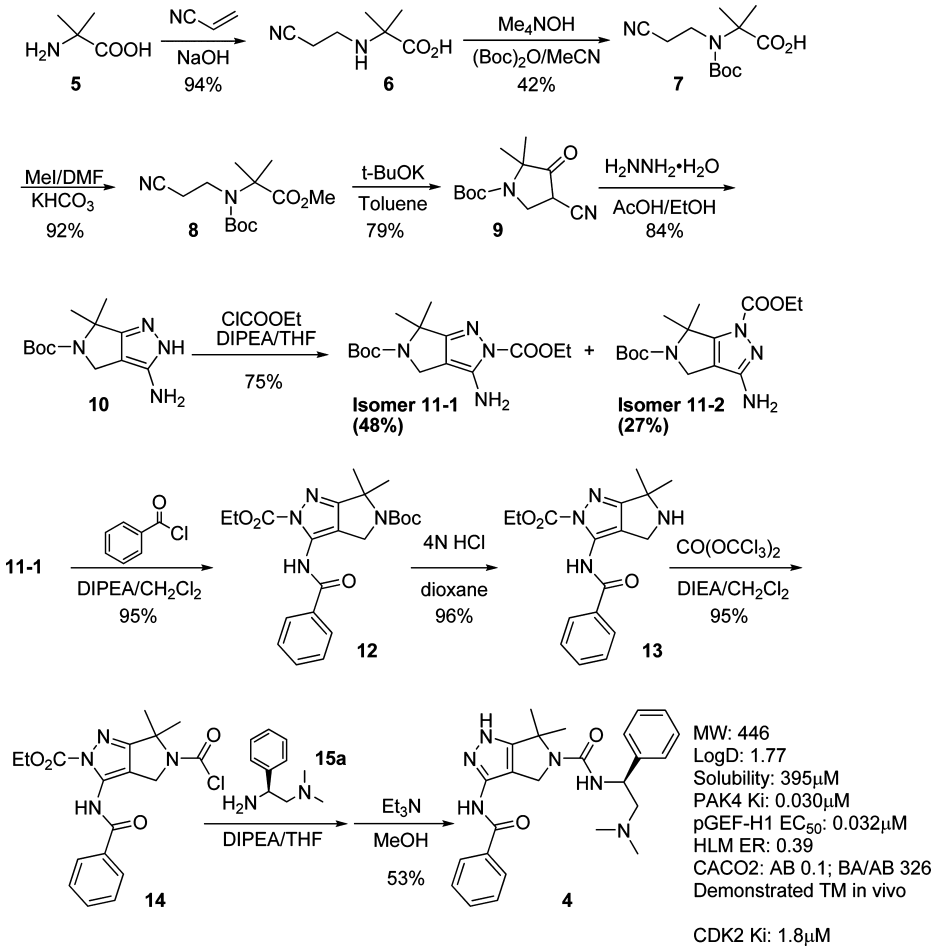

part of the ligand. Similarly, the phenoxy moiety of **3** is solvent-exposed and does not appear to contribute any specific interactions with the PAK4 protein. The head groups in both compounds maintain two key interactions, namely the charge−charge interaction to ASP-A458 and hydrophobic interaction (phenyl group in the head portion) with the glycine loop. The urea linker on the pyrrolopyrazole core seems to be a reasonable vector for positioning the phenylethyl diamine, the headgroup of **1**. On the basis of these observations, a new hybrid design of structure **4** (see Figure 3) was proposed which removed the unnecessary solvent exposed fragment (phenoxyl tail) and kept the key binding elements for potency: the geminal dimethyl groups, the phenyl moiety interacting with the glycine loop, and the basic amine in the head region. In addition, we felt that the pyrrolopyrazole template, with its less planar structural features, would likely be more selective toward PAK4 over other kinases than the flatter less selective benzimidazole indazole template of **1.**

Compound **4** (Scheme 1) was synthesized in five steps from key intermediate **11−1**, a versatile core protected deliberately with ethylcarbamoyl on one side and Boc on the other side. These orthogonal protecting groups allow a wide range of functional groups to be selectively attached to either side of the pyrrolopyrazole core. The key intermediate **11−1** was prepared by slightly modifying a previously described synthetic route.[18] Michael addition of 2-amino-2-methylpropanoic acid (**5**) to acrylonitrile afforded the amino acid **6** in 94% yield. The amino group of **6** was then protected as a Boc carbamate (**7**). The carboxylic acid **7** was converted to methyl ester **8** via treatment with iodomethane and potassium bicarbonate. The methyl ester **8** was cyclized under basic conditions to give **9** in 79% yield. The ketonitrile **9** was condensed with hydrazine under acidic conditions, affording the aminopyrazole **10** in 84% yield. The aminopyrazole **10** was reacted with ethylcarbamoyl chloride to give a mixture of two regioisomers, which could be separated by recrystallization or column chromatography. Both regioisomers (**11−1** and **11−2**) could be used for further derivatization effectively. With the improved procedure shown here, a large quantity (>250 g) of **11−1** and **11−2** can be obtained readily.[19] In the synthesis of **4**, the benzamide **12** was first established by acylation of the ethylcarbamoyl-protected aminopyrazole in **11−1**. The Boc group was then cleaved selectively to give amine **13**. Treatment of the amine **13** with triphosgene led to carbamoylchloride **14**, which is remarkably chemically stable, likely due to steric hindrance around the carbonyl. Even on large scale, the carbamoylchloride **14** could be obtained in excellent yield after aqueous workup and purification by normal phase column (silica gel) chromatography. The urea formation and deprotection of ethylcarbamoyl group could be done conveniently in a two-step, one-pot procedure, affording compound **4** in reasonable yield.

Compound **4** was found to be potent against PAK4 (Scheme 1) in both the enzymatic assay and the target-based cellular pGEF-H1 assays. The kinase selectivity profile was improved relative to the benzimidazole-indazole series. Compound **4** has 60-fold selectivity toward PAK4 relative to CDK2, whereas **1**

dx.doi.org/10.1021/jm300204j | J. Med. Chem. XXXX, XXX, XXX−XXX

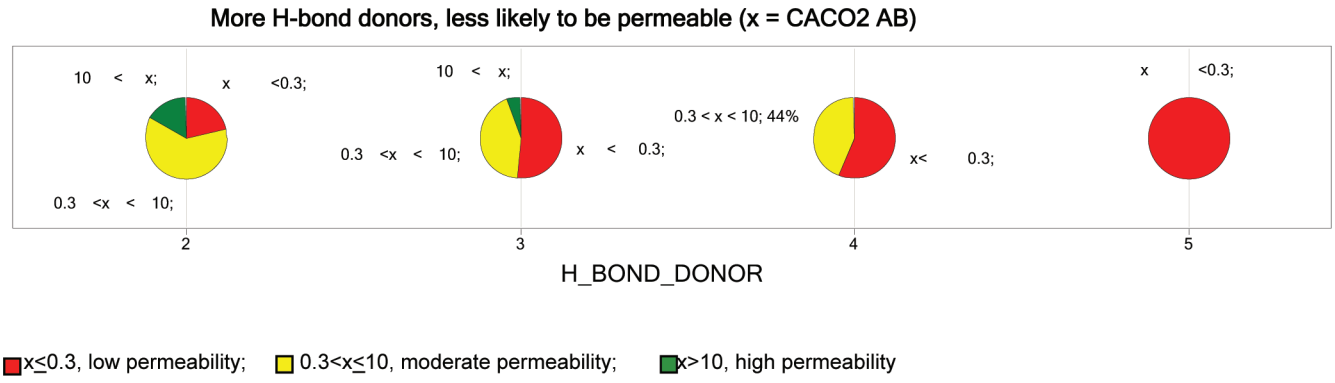

Figure 4. H-bond donors inversely correlate with permeability.

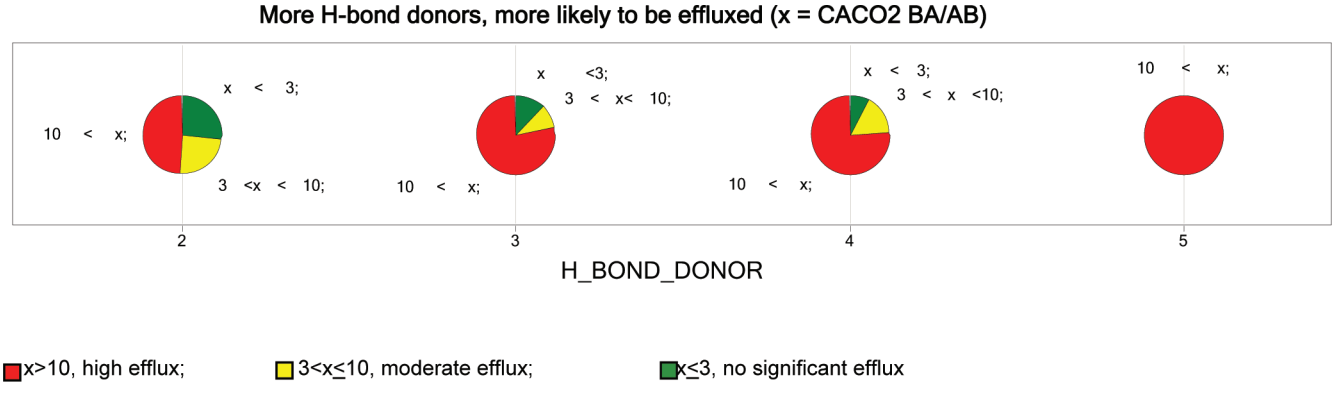

Figure 5. H-bond donors correlate with efflux.

favors CDK2 slightly over PAK4 in enzymatic assays. At a molecular weight of 446 and a measured log *D* of 1.77, compound **4** (LE = 0.32) is significantly more efficient than the original pyrrolopyrazole lead **3** (LE = 0.14). This new compound is also reasonably stable in human liver microsomes, with an extraction ratio of 0.39. The main issue for the compound is poor oral bioavailability, probably due to high efflux and/or poor permeability as suggested by CACO2 data.[20] Compound **4** was tested in an animal tumor model (HCT116) for pharmacodynamic target modulation (TM). To obtain sufficient drug exposure, the compound was dosed via continuous infusion from an implanted subcutaneous pump (80 mg/kg/day). At 18 h, pGEF-H1 was found to be down-regulated by ∼61% in tumors. The positive result increased our confidence in the ability of a small molecule to inhibit PAK4 in a tumor. The hybridized pyrrolopyrazole series became the focus of our subsequent chemistry effort, which aimed at improving oral absorption.

Efflux[20] seems to be the root cause of the observed poor oral absorption of **4** (CACO2 BA/AB: 326). The high efflux ratio may also make the flux from apical face to basolateral face appear to be artificially low (CACO2 AB: 0.1). The intrinsic permeability appears to be good, as suggested by high flux from basolateral face to apical face (BA: 32.6). To improve oral absorption, efflux needed to be reduced. Similar to permeability, efflux is known to generally correlate with polar surface area (PSA), charge, and number of hydrogen bond donors (NHBD) while inversely correlating with lipophilicity. Solubility is also a key factor. Low solubility can offset the benefits of increasing lipophilicity, and high solubility may help overcome efflux. Higher lipophilicity tends to be good for permeability but bad for solubility and therefore bad for achievable drug concentration. Low drug concentration due to poor solubility can limit passive permeability and contribute to efflux. Analysis of permeability data (CACO2 AB and BA)[20] vs physical properties (e.g., Log *P*, PSA, NHBD or kinetic solubility) for 784 existing pyrrolopyrazoles suggested that NHBD has the best correlation with permeability (inversely) and efflux. As shown in Figures 4 and 5, as the number of H-bond donors in a molecule increases from 2 to 5, the fraction of low permeability (CACO2 AB $\leq$ 0.3) compounds increases from 22% to 100% and the fraction of high efflux (CACO2 BA/AB > 10) compounds increases from 49% to 100%. Nonetheless, a significant challenge still existed because about half (49%) of the pyrrolopyrazoles with only two H-bond donors still demonstrated high efflux. For the pyrrolopyrazoles with three H-bond donors (e.g., compound **4**), the fraction with low permeability (CACO2 AB < 0.3) is substantial (51%) and the fraction with high efflux (CACO2 BA/AB > 10) is also high (78%). On the basis of this analysis, one of the resulting chemistry tactics was to remove hydrogen bond donors (HBD). Because the two aminopyrazole H-bond donors on the pyrrolopyrazole core are essential for binding, we first sought ways to block the urea NH in the head region.

Compounds **16** and **17** were synthesized via a route similar to the one used for compound **4** (Scheme 1). Simple methylation of the urea NH as in **16** led to significant loss of potency (Figure 6). Formation of the piperazine ring, as in **17**, gave molecules that retained most of the activities yet were metabolically unstable. Compounds **16** and **17** each have one less H-bond donor than compound **4**, but their permeability (CACO2 AB) improved only marginally and their efflux ratios (CACO2 BA/AB) remained high. In general, lipophilicity correlates inversely to metabolic stability within a chemical

dx.doi.org/10.1021/jm300204j | J. Med. Chem. XXXX, XXX, XXX−XXX

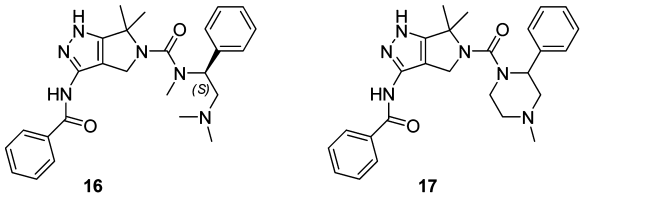

Figure 6. Blocking the urea NH resulted in modest reduction of efflux.

series. Because these molecules already had moderate metabolic stability, increasing the lipophilicity further to improve permeability did not seem like a reasonable strategy. Further reduction in the number of formal H-bond donors is likely challenging because the aminopyrazole is key binding element of this series.

Our next strategy was to reduce the overall molecular charge because it is known to decrease permeability and increase efflux. Cell membranes are made of phospholipid bilayers, which have evolved to be a barrier to passage of charged molecules foreign to cells. Highly charged molecules are also more likely to become substrates of efflux pumps (e.g., p-glycoproteins). Compound **4** possesses a basic amine with a pK_a of 9.01 (calculated with ACD-Lab 10.0), therefore, it is mostly protonated and charged (>97.5%) in the physiologic environment (pH ∼7.4). There are two different approaches that may be used to effect net charges: (1) lower the basicity to reduce the molecular charge or (2) completely replace the basic amine. Here, our attempts to modulate the basicity (pK_a of the amine) are described.

The initial design strategy was to add electron withdrawing groups on the phenyl ring in the headgroup of **4**, which fits tightly with the small hydrophobic pocket under the glycine-loop of PAK4 protein. Only small substituents such as cyano or fluoro were tolerated for binding (structures not shown). However, these analogues did not show any significant effect on efflux (CACO2 AB < 0.2), presumably because the substituents are too far from the amine to significantly reduce its basicity. Replacement of the phenyl ring with a pyridine led to large loss of potency (>50×, structures not shown).

Another design strategy to reduce the basicity of the amine was to replace the urea linker with a carbamate in the head region of **4**. Because oxygen is more electron-negative than nitrogen, the carbamate was believed to be more electron-withdrawing than the urea. The predicted basicity (pK_a by ACD-Lab 10.0) of the carbamate analogue **18** (Scheme 2) is 8.26, which is 0.75 log units lower than the pK_a (9.01) of compound **4**. The carbamate analogue also has one less H-bond donor and moderately higher lipophilicity (Log *D* 2.66 vs 1.77), which should enhance permeability. The carbamate analogues were synthesized from the chiral aminoalcohol **15b** and the carbamoyl chloride **14**/**14a**, which can be prepared readily via a route similar to the synthesis of **4**. As predicted, the carbamate analogue **18** experiences much less efflux (BA/AB ratio: 2.85 vs 326) than the urea analogue **4**. This design led to a dramatic reduction in efflux (∼100 fold). The carbamate analogues also retained all PAK4 inhibitory activities demonstrated by the urea analogue **4**. The carbamate on the pyrrolopyrazole core is stable chemically and metabolically, likely due to the steric hindrance vicinal to the carbonyl group. Hydrolysis of the carbamate was not detected when **19** was incubated in an acidic buffer (pH ∼2), basic buffer (pH ∼9), and human plasma. Unfortunately, these molecules (**18**−**19**) are otherwise generally unstable in HLM, making them unsuitable for a clinical development candidate (Scheme 2). In metabolite identification studies, demethylation was found to be a major metabolic pathway for these dimethylamines (both ureas and carbamates).

Compound **19** produced reasonable exposure in mice when dosed at 25 mg/kg orally. The resulting unbound drug concentration (unbound C_{av} ∼25 nM) remained above the cellular EC_{50} (pGEF-H1) for 8 h. The improved oral absorption enabled the evaluation of tumor growth inhibition (TGI) in a mouse xenograft model by oral route. After dosing 25 mg/kg twice a day orally for 15 days, compound **19** demonstrated significant TGI (∼61%) in the HCT116 human xenograft tumor model. Because HCT116 is a PAK4-driven tumor line,[12] the result increased our confidence in both PAK4 as an anticancer target and the pyrrolopyrazole as a viable chemical series.

Concurrent with our effort to reduce charge, another strategy was to reduce the number of effective H-bond donors. Effective H-bond donation discounts H-bonds that are internally satisfied or hindered. A tactic is to engineer in intramolecular H-bond interaction(s) to satisfy the existing H-bond donor(s), therefore reducing their exposure to solvent. This was achieved by introducing a fluorine, a methoxy, or an "aza" (2-pyridine) in the tail phenyl ring ortho to the amide (Figure 7). Although these substitutions had minimum effect on efflux for analogues with urea linker in head region (e.g., **20**), significant improvement was observed for analogues with the carbamate linker. For example, urea **20** has a high efflux ratio similar to urea **4**, whereas carbamate **21** has less efflux and is more permeable than carbamate **19**. At this point, among a number of our strategies aiming at reducing efflux of pyrrolopyrazoles, reduction of molecular charge was the most effective strategy

Scheme 2. Synthesis of Carbamates

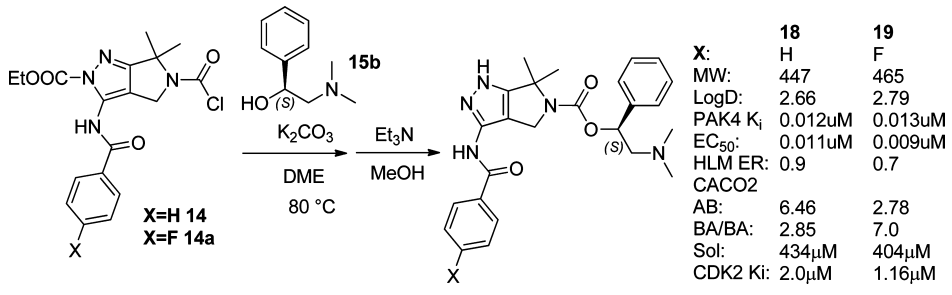

dx.doi.org/10.1021/jm300204j | J. Med. Chem. XXXX, XXX, XXX−XXX

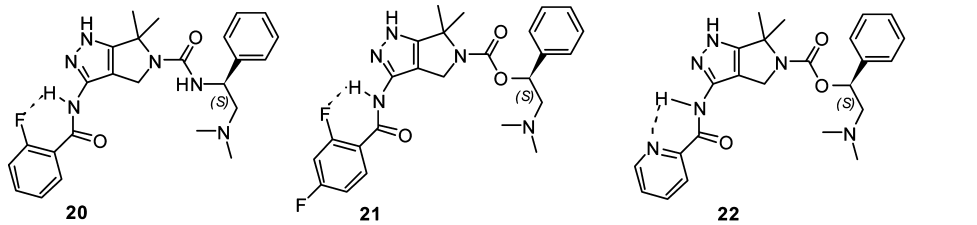

20
MW: 464
LogD: 2.33
PAK4 Ki: 0.098μM
pGEF-H1 EC_{50}: 0.036μM
HLM ER: 0.38
CACO2: AB 0.13; BA/AB 231

21
MW: 483
LogD: 2.68
PAK4 Ki: 0.068μM
pGEF-H1 EC_{50}: 0.015μM
HLM ER: 0.9
CACO2: AB 15.9; BA/AB 1.17

22
MW: 448
LogD: 2.23
PAK4 Ki: 0.031μM
pGEF-H1 EC_{50}: 0.028μM
HLM ER: 0.67
CACO2: AB 10.3; BA/AB 1.61

Figure 7. Internal H-bond reduced efflux marginally for ureas, significantly for carbamates.

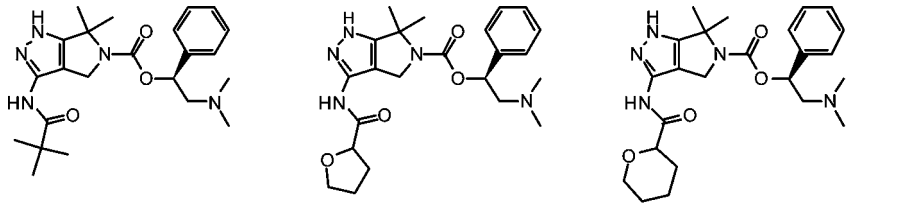

23
MW: 427
LogD: 2.52
pGEF-H1 EC_{50}: 0.004 uM
HLM ER: 0.44
CACO2: AB 1.70; BA/AB 9.9

24 (a mixture of diasteromers)
MW: 441
LogD: 2.08
pGEF-H1 EC_{50}: 0.016 uM
HLM ER: 0.4
CACO2: AB 1.84; BA/AB 8.7

25 (a mixture of diasteromers)
MW: 455
LogD: 2.48
pGEF-H1 EC_{50}: 0.018 uM
HLM ER: 1.0
CACO2: AB 5.26; BA/AB 3.6

Figure 8. Examples of small alkyl amides.

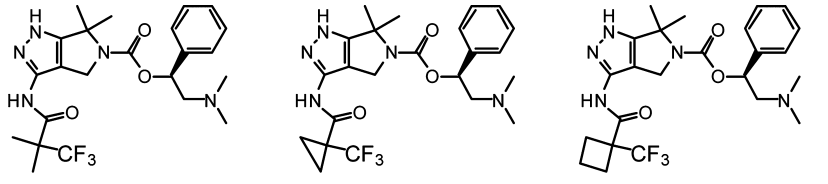

26
LogD: 1.61
pGEF-H1 EC_{50}: 0.001 uM
HLM ER: 0.55
PAMPA: 8

27
LogD: 1.50
pGEF-H1 EC_{50}: 0.007 uM
HLM ER: 0.42
PAMPA: 23

28
LogD: 1.60
pGEF-H1 EC_{50}: <0.001 uM
HLM ER: 0.6
PAMPA: 7

Figure 9. Examples of fluorinated alkyl amides.

followed by lowering the number of both formal or/and effective H-bond donors. Increasing lipophilicity can be beneficial for permeability and lowering efflux but can also be limited by its potential negative impact on metabolic stability.

The pyridine analogue, **22**, was one of the more metabolically stable carbamates, presumably due to its lower lipophilicity than other carbamates such as **18**, **19**, and **21**. The compound also has a reasonable overall in vitro profile; it is potent, soluble, and permeable without efflux. Unfortunately, rat PK study revealed low oral bioavailability and high clearance. Because the liver microsome extraction ratio of **22** is still relatively high (HLM ER 0.67), an improved metabolic stability was sought.

From cocrystal structures of **3** and other compounds, we observed that the aryl amide moiety was not making interactions that required an aromatic group (such as $\pi-\pi$ stacking). We speculated that a small bulky alkyl group could make similar, if not better, lipophilic interactions with the PAK4 protein. Analogues containing a number of these alkyl amides were made and found to have better metabolic stability than the aromatic amides despite having similar lipophilicities. This was a distinct advantage in the carbamate subseries, where we could maintain permeability but needed stability. The *t*-butyl amide compound, **23** (Figure 8), was an example of a compound with a desirable combination of attributes. It is potent in the cellular assay, reasonably permeable, and metabolically stable. As compared to **18**, an aryl amide analogue with comparable lipophilicity and activity, **23** shows much better metabolic stability, slightly less permeability, and slightly more efflux.

The tactic of improving permeability for the alkyl amides by masking an H-bond donor through designed an intramolecular H-bond gave mixed results. When oxygen ethers are used to form the intramolecular H-bond, permeability increased and efflux decreased in most cases, however, inherent metabolic stability also decreased. (Figure 8, **24** and **25**).[21] The tetrahydrofuran analogue **24** has similar permeability, efflux and metabolic stability as **23** despite having lower lipophilicity (log *D* 2.08 vs log *D* 2.52). Tetrahydropyran **25** has similar

dx.doi.org/10.1021/jm300204j | *J. Med. Chem.* XXXX, XXX, XXX−XXX

lipophilicity (log *D* 2.48) to **23** but has much better permeability and less efflux. A possible cause is that the tetrahydropyran masks the amide NH better than the tetrahydrofuran. However, the metabolic stability of **25** is significantly worse (HLM ER = 1.0) than **23** or **24**. Overall, the oxygenated alkyl amides proved to be less active and less stable than their carbon alkyl counterparts.

Another tactic is to use trifluoromethyl groups and rigid small carbocycles to attenuate the lipophilicity of **23** and improve its metabolic stability. Switching one of the *t*-butyl amide methyl groups for a trifluoromethyl group led to **26** (Figure 9). This compound shows a significant increase in PAK4 activity over **23** and is significantly less lipophilic. So it came as somewhat of a surprise when its metabolic stability was shown to be slightly worse. Reducing the lipophilicity further by forming a 3-member cyclopropyl ring between the two remaining methyl groups (**27**) resulted in a compound with a very similar in vitro profile to **23** even though its lipophilicity is a log unit lower. Creating the 4-member cyclobutyl ring analogue (**28**) resulted in a very potent compound with similar lipophilicity to the trifluoromethyl *t*-butyl amide **26** but significantly worse metabolic stability. The trifluoromethyl group did lower the lipophilicity and maximize ligand−protein hydrophobic interactions, resulting in more potent PAK4 inhibitors. However, metabolic stability of the molecules did not track with the lipophilicity as expected. A metabolite identification study on compounds **23** and **26** suggested that its major metabolite is de-alkylation product of the dimethylamine. The above modifications (fluorination) remote from the soft spot appeared to be ineffective in decreasing the metabolism.

Because of the improved in vitro profile of the alkyl amides (e.g., **23**, **24**, **26**, and **27**) over the aryl amides (e.g., **19** and **22**), these molecules were tested in rat PK studies (Table 1). The

Table 1. Rat PK Data of Selected Pyrrolopyrazoles

compd	dose (mg/kg) IV/PO	clearance (mL/min/kg)	Vds (L/kg)	$T_{1/2}$ (h)	F_{po} (%)
19	5/10	98	6.1	1.1	9
22	5/10	146	4.8	0.7	2
23	5/10	52	2.8	0.8	15
24	5/10	69	2.2	0.5	20
26	5/10	37	4.3	1.3	45
27	5/10	24.1	2.8	1.5	46

alkyl amides analogues overall showed better oral bioavailability in the rat oral PK (F_{po} = 15−46%) compared to the aryl amide analogues (F_{po} = 9% and 2%). The two alkyl amides, **23** and **24**, have moderate oral bioavailability along with high in vivo clearance in rats (52 and 69 mL/min/kg, respectively) resulting in shorter half-lives. On the other hand, the fluoroalkyl amide analogues, **26** and **27** demonstrated good oral bioavailability and have low to moderate in vivo clearance (37 and 24 mL/min/kg, respectively), which is a significant improvement.

The pharmacokinetics of **23** were further evaluated in dog. In this animal model, **23** had moderate oral bioavailability of 20%, low clearance of 12 mL/min/kg, and a half-life of 2.2 h. On the basis of these encouraging ADME properties, two of the alkyl amide analogues, **23** and **26**, were selected for further evaluation in our in vivo antitumor efficacy models. **23** demonstrated efficacy in a HCT-116 xenograft tumor mouse model. At a dose of 20 mpk bid (**23**), significant tumor growth inhibition (TGI = 52%) was observed. In an M24 xenograft tumor model, containing a cell line where phosoPAK4 is up-regulated,[13] **23** and **26** showed excellent tumor growth inhibition (TGI) with oral dosing (see Table 2 and Figure 10). These results show that the alkyl amide analogues such as **23** and **26** are effective PAK4 inhibitors that can inhibit tumor growth in vivo in PAK4-driven cell lines.

Table 2. Efficacy of PAK4 Inhibitors in Tunor Xenograft Mouse Models

efficacy (TGI) of PAK4 inhibitors	**19** (dose, free Cave)	**23** (dose, free Cave)	**26** (dose, free Cave)
HCT-116 (colon)	12% (50 mg/kg sid, 70 nM)	37% (12.5 mg/kg bid, nd)	NT
	61% (25 mg/kg bid, 25 nM)	52% (20 mg/kg bid, nd)	
$M24^{met}$ (melanoma)	NT	41% (3.75 mg/kg bid, 5.3 nM)	67% (7.5 mg/kg bid, 13.9nM)
		61% (7.5 mg/kg bid, 28.3 nM)	87% (15 mg/kg bid, 31nM)
		68% (15 mg/kg bid, 50.5 nM)	

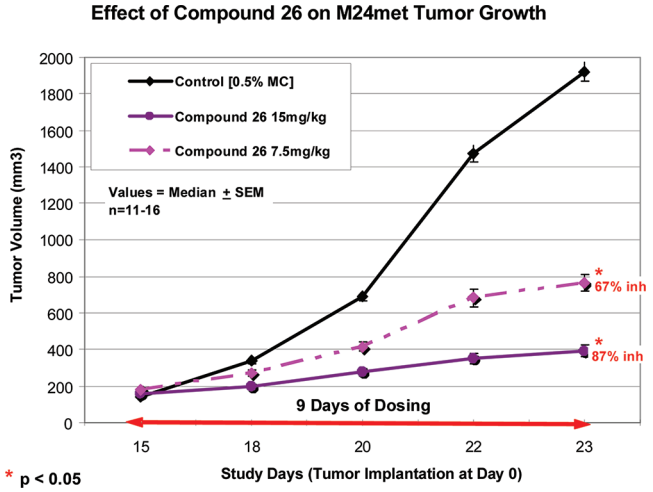

Figure 10. Oral efficacy of **26** in melanoma xenograft tumor mouse model.

Compound **23** was evaluated towards endogenous human protein kinases using ActivX's affinity labeling method. Of the 174 kinases identified with the ADP affinity probe, only 4 other kinases were inhibited to a significant degree (>40%): PKD3, ERK1, GSK3β, PCTAIRE. When the ATP affinity probe was used to enlarge the number of studied protein kinases to 266 total kinases, additional potential kinase activities were detected (cdk7, Erk5, MST3, MARK2). Using recombinant protein from multiple kinase screening services (University of Dundee, Invitrogen, Pfizer-internal) both compounds **23** and **26** were found to be selective inhibitors. Of the 119 unique protein kinases screened at 1000 nM, only a small cohort showed significant (>70%) inhibition: AMPK, cdk7, Erk2, PBK, GSK3β, RSK, PKA, MARK, MST4. When follow-up dose-response analysis was undertaken, **23** was shown to have moderate-to-modest inhibition on a subset of the screening hits: cdk2 (IC_{50} = 450 nM), GSK3β (IC_{50} = 227 nM), ERK2 (IC_{50} = 170 nM), MARK1 (IC_{50} = 115 nM). As such, compounds **23** and **26** are highly PAK-specific inhibitors.

dx.doi.org/10.1021/jm300204j | *J. Med. Chem.* XXXX, XXX, XXX−XXX

CONCLUSION

In summary, the combination of SBDD, traditional, and novel medicinal chemistry principles led to the identification of a novel, potent, and selective PAK4 inhibitor (**4**), which demonstrated target modulation in a PAK4 driven tumor model. This novel series was optimized for reduced efflux utilizing medicinal chemistry strategies. While reducing the number of hydrogen bond donors resulted in moderate benefit, lowering the molecular charge was found to be more effective in reducing efflux for this series of PAK4 inhibitors. These strategies ultimately led to the discovery of a number of orally bioavailable PAK4 inhibitors (e.g., **13**, **23**, and **26**). Of these, two compounds were shown to potently inhibited tumor growth in PAK4-driven (HCT116 and M24^{met}) tumor xenograft models through oral dosing providing additional support for PAK4 as an attractive oncology target for therapeutic benefit to cancer patients.[13]

EXPERIMENTAL SECTION

Syntheses of Compounds. Starting materials and other reagents were purchased from commercial suppliers and were used without further purification unless otherwise indicated. All reactions were performed under a positive pressure of nitrogen, argon, or with a drying tube, at ambient temperature (unless otherwise stated), and in anhydrous solvents, unless otherwise indicated. The reactions were assayed by high-performance liquid chromotagraphy (HPLC) or thin-layer chromatography (TLC) and terminated as judged by the consumption of starting material. Analytical thin-layer chromatography was performed on glass-backed silica gel 60 F_{254} plates (EMD, 0.25 mm) and eluted with the appropriate solvent ratios (v/v). The TLC plates were visualized by UV, phosphomolybdic acid stain, or iodine stain. Flash column chromatography was performed using glass columns packed with 60 Å silica gel (200−400 mesh) or with Biotage Flash Si prepacked cartridges. For chromatography of basic compounds, ammonia-saturated methanol (made by bubbling ammonia gas into a 4 L bottle of methanol for 1 h) or a mixture of 5% concentrated ammonium hydroxide in 95% ethanol were mixed with less polar cosolvents in the mobile phase. Alternatively, reverse-phase preparative HPLC was used (Dionex prep-HPLC: Column, Hi-Q_C18 150 mm × 20 mmID; solvent, MeCN/water +0.1% TFA or HOAc). Proton NMR spectra were collected on 300, 400, or 700 MHz spectrometers as indicated, and chemical shifts are reported in parts per million (ppm) relative to the designated referenced peaks: $CDCl_3$ 7.27 ppm, DMSO-d_6 2.50 ppm, CD_3OD 3.31 ppm, D_2O 4.75 ppm. When peak multiplicities are reported, the following abbreviations are used: s = singlet, d = doublet, t = triplet, m = multiplet, br = broadened, dd = doublet of doublets, dt = doublet of triplets, ddd = doublet of double doublets. Coupling constants, when given, are reported in hertz. The NMR spectra of many of the final compounds showed mixtures of tautomeric isomers, resulting in doubling of signals for certain protons. In these cases, the shifts and multiplicities corresponding to the major tautomer are given.

Analytical mass spectra were obtained using liquid chromatography mass spectrometry (LC-MS) on an Agilent instrument using atmospheric pressure chemical ionization (APCI) or electrospray ionization (ESI). High-resolution mass spectra (HRMS) were obtained from an Agilent TOF 6200 series with ESI. Elemental microanalyses were performed by Atlantic Microlabs Inc., Norcross, GA, and gave results for the elements stated within ±0.4% of the theoretical values. The purity of all final compounds was determined to be at least 95% pure by a combination of HPLC, LCMS, NMR (no extra peaks in the proton NMR spectrum), combustion analysis (all final compounds have satisfying CHN results consistent with high purity), and HRMS.

2-(2-Cyanoethylamino)-2-methylpropanoic Acid (6). To a slurry of 2-amino-2-methylpropanoic acid (2020 g, 19.8 mol) in water (1.7 L) at 0 °C was added a solution of sodium hydroxide (792 g, 19.8 mol) in water (1.8 L) while maintaining the temperature below 15 °C, followed by addition of acrylonitrile (1050 g, 19.81 mol). After addition, the mixture was stirred at room temperature overnight. The reaction mixture was acidified to pH ∼3 with concd HCl (1.7 L), causing a precipitate to form. The solution was filtered, and the solid precipitate was dried in oven at 45 °C for 2 days to afford crude acid **6** (2900 g, 94%) as a white solid, which was used in the next step without further purification. ^{1}H NMR (400 MHz, D_2O) δ ppm 1.45 (s, 6H), 2.95 (t, J = 6.8 Hz, 2H), 3.32 (t, J = 6.8 Hz, 2H).

2-(*tert*-Butoxycarbonyl(2-cyanoethyl)amino)-2-methylpropanoic Acid (7). To a suspension of amine **6** (1.3 kg, 8.32 mol) in acetonitrile (10 L) was added 25% aqueous tetramethylammonium hydroxide (3.33 kg, 9.15 mol), resulting in a clear solution. To the solution was added di-*tert*-butyl dicarbonate (4.54 kg, 20.8 mol) portionwise over 5 h. After the addition was complete, the mixture was stirred at 50 °C for two days. After evaporation of solvents, the residue was dissolved in water (20 L) and extracted with ethyl acetate (2 × 10 L) to remove residual di-*tert*-butyl dicarbonate. The aqueous layer was acidified with solid citric acid to pH 4−5 and extracted with ethyl acetate (3 × 15 L). The combined organic layers were washed with brine (2 × 4 L), dried over sodium sulfate, and concentrated to dryness, leaving acid **7** (860 g, 42%) as a white solid. ^{1}H NMR (400 MHz, chloroform-*d*) δ ppm 1.44 (s, 9H), 1.54 (s, 6H), 2.67 (t, J = 6.8 Hz, 2H), 3.62 (t, J = 6.8 Hz, 2H).

Methyl 2-(*tert*-Butoxycarbonyl(2-cyanoethyl)amino)-2-methylpropanoate (8). Iodomethane (1979 g, 13.9 mmol) was added dropwise to a room temperature mixture of acid **7** (1780 g, 6.95 mol) and potassium bicarbonate (2085 g, 20.85 mol) in dimethylformamide (8.5 L). After addition was complete, the mixture was heated to 40 °C and stirred at that temperature overnight. After cooling to room temperature, saturated aqueous ammonium chloride solution (3 L) and water (15 L) were added. The mixture was extracted with ethyl acetate (3 × 4 L). The combined organic layers were washed with brine (4 × 5 L), dried over sodium sulfate, and concentrated in vacuo to give ester **8** (1720 g, 92%) as a yellow solid. ^{1}H NMR (400 MHz, chloroform-*d*) δ ppm 1.42 (s, 9H), 1.50 (s, 6H), 2.65 (t, J = 6.8 Hz, 2H), 3.60 (t, J = 6.8 Hz, 2H), 3.69 (s, 3H).

***tert*-Butyl 4-Cyano-2,2-dimethyl-3-oxopyrrolidine-1-carboxylate (9).** To a cooled (0 °C) solution of ester **8** (860 g, 3.185 mol) in toluene (10 L) was added potassium *tert*-butoxide (463 g, 4.14 mol), and the resulting mixture stirred at 5 °C overnight. Glacial acetic acid (280 mL) was added, and then the mixture was partitioned between water (5 L) and ethyl acetate (10 L). The organic layer was washed with brine (2 × 5 L), dried over sodium sulfate, and concentrated in vacuo. The residue was recrystallized from ether/petroleum ether (50 mL/2 L) to give compound **9** (600 g, 79%) as a white solid. ^{1}H NMR (400 MHz, chloroform-*d*) δ ppm 1.46 (s, 3H), 1.48 (s, 3H), 1.51 (s, 9H), 3.61−3.71 (m, 2H), 4.22 (br m, 1H).

***tert*-Butyl 3-Amino-6,6-dimethyl-4,6-dihydropyrrolo[3,4-*c*]pyrazole-5(2*H*)-carboxylate (10).** Hydrazine monohydrate (804.6 mL, 16.54 mol) was added dropwise to a room temperature solution of compound **9** (761 g, 3.087 mol) and glacial acetic acid (1475 mL, 25.74 mol) in anhydrous ethanol (10.75 L). The mixture was stirred at reflux for 12 h. The solvents were evaporated and the residue taken up in ethyl acetate (9 L) and water (8 L). The biphasic mixture was basified to pH ∼8 with solid potassium carbonate (649 g, 4.7 mol). The layers were separated, and the aqueous layer was extracted further with ethyl acetate (2 × 4 L). The combined organic extracts were washed with brine (2 × 4 L), dried over sodium sulfate, and concentrated to dryness, giving crude compound **10** (750 g, 84%) as a yellow sticky solid. ^{1}H NMR shows the molecule as a mixture of 1*H* and 2*H* tautomers, exact ratio depending on solvent and concentration. ^{1}H NMR (400 MHz, DMSO-d_6) δ ppm 1.42 and 1.45 (2 s, 9H), 1.49 and 1.51 (2 s, 6H), 4.08 and 4.12 (2 s, 2H), 4.92 (br s, 2H), 11.15 (br s, 1H).

5-*tert*-Butyl 2-Ethyl 3-Amino-6,6-dimethylpyrrolo[3,4-*c*]pyrazole-2,5(4*H*,6*H*)-dicarboxylate (11−1) and 5-*tert*-Butyl 1-Ethyl 3-Amino-6,6-dimethylpyrrolo[3,4-*c*]pyrazole-1,5(4*H*,6*H*)-dicarboxylate (11−2). A solution of **10** (793 g, 3.14 mol) and diisopropylethyl amine (812 g, 6.28 mol) in tetrahydrofuran (13 L)

dx.doi.org/10.1021/jm300204j | J. Med. Chem. XXXX, XXX, XXX−XXX

was cooled to 0 °C. A solution of ethyl chloroformate (340 g, 3.14 mol) in tetrahydrofuran (0.98 L) was added dropwise over 2.5 h. The reaction was allowed to warm to room temperature as it was stirred for 2 h until no trace of **10** was visible by TLC (silica, 5%MeOH/DCM, UV visualization). Two product isomers are visible by TLC: the major isomer with R_f ~0.7, and the minor isomer with R_f ~0.3 (5%MeOH/DCM). The solvents were evaporated under reduced pressure. The residue was dissolved in dichloromethane (10 L) and washed with water (10 L, then 2 × 4 L) to remove DIPEA·HCl. The organic layer was dried with magnesium sulfate, decolorized with charcoal, filtered, and concentrated not quite to dryness (leaving some dichloromethane), to obtain a yellow oil. Ethyl ether (2 L) was added and the solution stirred for 2 h. The resulting suspension was filtered, and the light-brown precipitate rinsed with cold ether (650 mL). The filtrate and ether rinse were saved for later. The solid precipitate (still a mixture of isomers by TLC) was dissolved in dichloromethane, concentrated to a small volume, and the residue stirred in ether (2 L) for 3 h. The resulting white precipitate (single isomer by TLC) was collected by filtration and rinsed with cold ether (650 mL). The filtrate and ether rinse were saved for later. The precipitate (major isomer only by TLC) was dried in a vacuum oven at 40−45 °C.

The reserved filtrates from above were concentrated to dryness, the residue dissolved in dichloromethane and concentrated again to a small volume of yellow oil. The oil was stirred in ether (1 L) for 3 h, and the resulting precipitate (minor isomer only by TLC) was collected by filtration and rinsed with cold ether (500 mL). A second crop was obtained from the filtrate by the same procedure. The crops were combined and dried in a vacuum oven at 40−45 °C.

The remaining filtrate (~1:1 mixture of isomers by TLC) was purified by silica gel chromatography, eluting with 0−5% methanol in dichloromethane. The separated isomers obtained from the column were combined with their corresponding precipitate crops and dried to constant volume.

The major, less-polar isomer **11−1** (487 g, 48%) was obtained as a white solid, mp 199−201 °C. ^{1}H NMR shows the molecule as a mixture of rotamers: ^{1}H NMR (400 MHz, chloroform-*d*) δ ppm 1.46 (t, *J* = 7.20 Hz, 3 H), 1.49 and 1.53 (2 s, 9H), 1.66 and 1.71 (2 s, 6H), 4.23 and 4.28 (2 s, 2H), 4.51 (q, *J* = 7.24 Hz, 2H), 5.35 and 5.45 (2 br s, 2H).

The minor, more polar isomer **11−2** (278 g, 27%) was obtained as white crystals, mp 175−177 °C. ^{1}H NMR shows the molecule as a mixture of rotamers: ^{1}H NMR (400 MHz, chloroform-*d*) δ ppm 1.44 (t, *J* = 7.07 Hz, 3H), 1.48 and 1.53 (2 s, 9H), 1.76 and 1.82 (2 s, 6H), 4.01 and 4.07 (2 br s, 2H), 4.26 and 4.29 (2 s, 2H), 4.46 (q, *J* = 7.24 Hz, 2H).

5-*tert*-Butyl 2-Ethyl 3-Benzamido-6,6-dimethylpyrrolo[3,4-*c*]pyrazole-2,5(4*H*,6*H*)-dicarboxylate (12). A solution of benzoyl chloride (5.75 g, 40.7 mmol) in dichloromethane (50 mL) was added dropwise to a cooled (0 °C) and stirred solution of 5-*tert*-butyl 2-ethyl 3-amino-6,6-dimethylpyrrolo[3,4-*c*]pyrazole-2,5(4*H*,6*H*)-dicarboxylate **11−1** (12.0 g, 37.0 mmol) and diisopropylethyl amine (13.0 mL, 74.0 mmol) in dichloromethane (100 mL). The resulting clear solution was stirred at room temperature for 12 h. The reaction mixture was washed with water (2 × 75 mL), dried over sodium sulfate, filtered, and concentrated. The residue was purified by silica gel chromatography, eluting with 40% ethyl acetate in hexanes, to give amide **12** (15.0 g, 95%) as an off-white solid. ^{1}H NMR (300 MHz, $CDCl_3$) δ ppm 1.44−1.56 (m, 12H), 1.69 (s, 3H), 1.75 (s, 3H), 4.58 (q, *J* = 7.10 Hz, 2H), 4.74 (s, 1H), 4.79 (s, 1H), 7.44−7.64 (m, 3H), 7.87−7.96 (m, 2H), 10.97−11.11 (m, 1H).

Ethyl 3-Benzamido-6,6-dimethyl-5,6-dihydropyrrolo[3,4-*c*]-pyrazole-2(4*H*)-carboxylate (13). To a stirred slurry of intermediate **12** (15.0 g, 35.0 mmol) in ethanol (150 mL) was dropwise added 4 M HCl solution in dioxane (44 mL). The resulting clear solution was stirred at room temperature for 12 h. The reaction mixture was concentrated to dryness under vacuum and the residue stirred with hexane (250 mL) for 10 min. The solid product was collected by filtration, washed with hexane (100 mL), and dried under vacuum at 40 °C for 15 h to give the dihydrochloride salt of amine **13** (13.5 g, 96%), an off-white solid. ^{1}H NMR (300 MHz, DMSO-d_6) δ ppm 1.36 (t, *J* = 6.97 Hz, 3H), 1.67 (s, 6H), 4.47 (q, *J* = 7.16 Hz, 2H), 4.59 (s, 2H), 7.55−7.74 (m, 3H), 7.92 (d, *J* = 7.54 Hz, 2H), 10.23 (s, 2H), 10.93 (s, 1H). HRMS: $[M + H]^+$ calcd 329.160817, found 329.16117, error 1.07 ppm.

Ethyl 3-Benzamido-5-(chlorocarbonyl)-6,6-dimethyl-5,6-dihydropyrrolo[3,4-*c*]pyrazole-2(4*H*)-carboxylate (14). To a cooled (−10 °C) and stirred mixture of triphosgene (7.2 g, 24.3 mmol) and dihydrochloride salt **13** (13.0 g, 32.5 mmol) in dichloromethane (150 mL) was added a solution of diisopropylethyl amine (28.4 mL, 162.5 mmol) in dichloromethane (50 mL) over a period of 15 min. The resulting solution was stirred at 0 °C for 30 min. The reaction mixture was washed with water (2 × 100 mL), dried over sodium sulfate, filtered, and concentrated. The crude product was stirred with 25% ethyl acetate in hexane and the resulting precipitate collected by filtration and dried under vacuum at 40 °C to give carbonyl chloride **14** (12 g, 95%) as white solid. ^{1}H NMR (300 MHz, chloroform-*d*) δ ppm 1.51 (t, *J* = 7.06 Hz, 3H), 1.75−1.84 (m, 6H), 4.60 (q, *J* = 7.03 Hz, 2H), 5.08 (s, 2H), 7.46−7.69 (m, 3H), 7.85−7.98 (m, 2H), 11.10 (s, 1H). Anal. ($C_{18}H_{19}ClN_4O_4 \cdot 0.3H_2O$) C, H, N, Cl. HRMS: $[M + H]^+$ calcd 391.116759, found 391.117542, error 2.0 ppm.

A similar three-step procedure was used to make the following seven compounds:

Ethyl 5-(Chlorocarbonyl)-3-(4-fluorobenzamido)-6,6-dimethyl-5,6-dihydropyrrolo[3,4-*c*]pyrazole-2(4*H*)-carboxylate (14a). ^{1}H NMR (300 MHz, chloroform-*d*) δ ppm 1.50 (t, *J* = 7.16 Hz, 3H), 1.79 (s, 6H), 4.60 (q, *J* = 7.10 Hz, 2H), 5.06 (s, 2H), 7.16−7.24 (m, 2H), 7.89−7.98 (m, 2H), 11.07 (s, 1H). Anal. ($C_{18}H_{18}ClFN_4O_4 \cdot 0.15H_2O$) C, H, N, Cl, F.

Ethyl 5-(Chlorocarbonyl)-3-(2-fluorobenzamido)-6,6-dimethyl-5,6-dihydropyrrolo[3,4-*c*]pyrazole-2(4*H*)-carboxylate (32). ^{1}H NMR (300 MHz, chloroform-*d*) δ ppm 1.49 (t, *J* = 7.06 Hz, 3H), 1.72−1.85 (m, 6H), 4.60 (q, *J* = 7.10 Hz, 2H), 5.07 (s, 2H), 7.17−7.24 (m, 1H), 7.28−7.38 (m, 1H), 7.52−7.64 (m, 1H), 8.08−8.19 (m, 1H), 11.42 (d, *J* = 13.19 Hz, 1H). Anal. ($C_{18}H_{18}ClFN_4O_4 \cdot 0.2HCl$) C, H, N, Cl, F.

Ethyl 5-(Chlorocarbonyl)-3-(2,4-difluorobenzamido)-6,6-dimethyl-5,6-dihydropyrrolo[3,4-*c*]pyrazole-2(4*H*)-carboxylate (33). ^{1}H NMR (300 MHz, chloroform-*d*) δ ppm 1.44−1.56 (m, 3H), 1.74−1.84 (m, 6H), 4.60 (q, *J* = 7.16 Hz, 2H), 5.06 (s, 2H), 6.89−7.14 (m, 2H), 8.09−8.28 (m, 1H), 11.37 (d, *J* = 13.00 Hz, 1H). Anal. ($C_{18}H_{17}ClF_2N_4O_4$) C, H, N, Cl, F.

Ethyl 5-(Chlorocarbonyl)-6,6-dimethyl-3-(picolinamido)-5,6-dihydropyrrolo[3,4-*c*]pyrazole-2(4*H*)-carboxylate (34). ^{1}H NMR (400 MHz, chloroform-*d*) δ ppm 1.54 (t, *J* = 7.07 Hz, 3H), 1.83 (s, 6H), 4.65 (q, *J* = 7.07 Hz, 2H), 5.12 (s, 2H), 7.56 (ddd, *J* = 7.64, 4.74, 1.26 Hz, 1H), 7.95 (td, *J* = 7.77, 1.64 Hz, 1H), 8.26 (d, *J* = 7.83 Hz, 1H), 8.75 (d, *J* = 4.04 Hz, 1H), 12.31 (s, 1H).

Ethyl 5-(Chlorocarbonyl)-6,6-dimethyl-3-pivalamido-5,6-dihydropyrrolo[3,4-*c*]pyrazole-2(4*H*)-carboxylate (35). ^{1}H NMR (400 MHz, DMSO-d_6) δ ppm 1.22 (s, 9H), 1.35 (t, *J* = 7.1 Hz, 3H), 1.64 (s, 6H), 4.45 (q, *J* = 7.1 Hz, 2H), 4.85 (s, 2H), 10.28 (s, 1H). Anal. ($C_{16}H_{23}ClN_4O_4$) C, H, N, Cl.

Ethyl 5-(Chlorocarbonyl)-6,6-dimethyl-3-(tetrahydrofuran-2-carboxamido)-5,6-dihydropyrrolo[3,4-*c*]pyrazole-2(4*H*)-carboxylate (36). ^{1}H NMR (400 MHz, DMSO-d_6) δ ppm 1.35 (t, *J* = 7.1 Hz, 3H), 1.64 (d, *J* = 2.3 Hz, 6H), 1.86 (m, 2H), 1.98 (m, 1H), 2.23 (m, 1H), 3.91 (m, 2H), 4.45 (m, 3H), 4.87 (s, 2H), 10.84 (s, 1H). Anal. ($C_{16}H_{21}ClN_4O_5 \cdot 0.15H_2O$) C, H, N, Cl.

Ethyl 5-(Chlorocarbonyl)-6,6-dimethyl-3-(tetrahydro-2*H*-pyran-2-carboxamido)-5,6-dihydropyrrolo[3,4-*c*]pyrazole-2(4*H*)-carboxylate (37). ^{1}H NMR (400 MHz, DMSO-d_6) δ ppm 1.35 (t, *J* = 7.1 Hz, 3H), 1.38 (m, 1H), 1.53 (m, 3H), 1.64 (s, 6H), 1.81 (m, 1H), 1.98 (m, 1H), 3.55 (m, 1H), 4.04 (m, 2H), 4.43 (q, *J* = 7.1 Hz, 2H), 4.87 (s, 2H), 10.76 (s, 1H). Anal. ($C_{17}H_{23}ClN_4O_5$) C, H, N, Cl.

(*S*)-N^1,N^1-Dimethyl-2-phenylethane-1,2-diamine (15a). To a mixture of (*S*)-2-(benzyloxycarbonylamino)-2-phenylacetic acid (196 g, 688 mmol), *O*-benzotriazole-*N*,*N*,*N*′,*N*′-tetramethyl-uronium-hexafluoro-phosphate (HBTU) (261 g, 688 mmol), and dichloromethane (2.8 L) were added sequentially potassium carbonate (285 g, 2.06

dx.doi.org/10.1021/jm300204j | J. Med. Chem. XXXX, XXX, XXX−XXX

mol) and dimethylamine hydrochloride (84.1 g, 1031 mmol). The reaction mixture was heated at 40 °C overnight. After cooling to room temperature, the solids were filtered, washed with ethyl acetate (2 × 500 mL), and the filtrate concentrated to a residue. Water (1 L) was added to the residue and the mixture agitated in an ultrasonic cleanser for 2 h. The precipitated solids were collected and washed with water (4 × 300 mL), washed with hexane (2 × 500 mL), and then dried under vacuum for 24 h. The solid crude product was dissolved in chloroform (300 mL), and undissolved solids were filtered off. The filtrate was concentrated to dryness and the residue dissolved in 2:1 hexane/ethyl acetate (250 mL) and allowed to stand at room temperature overnight. The resulting crystals were collected by filtration, washed with 3:1 hexane/ethyl acetate (100 mL), and dried in high vacuum at 40 °C for 24 h to give (*S*)-benzyl 2-(dimethylamino)-2-oxo-1-phenylethylcarbamate (100.0 g, 47%) as a white crystalline solid. ^{1}H NMR (300 MHz, $CDCl_3$) δ ppm 2.88 (s, 3H), 2.98 (s, 3H), 5.01 (d, J = 12.2 Hz, 1H), 5.11 (d, J = 12.2 Hz, 1H), 5.58 (d, J = 7.5 Hz, 1H), 6.37 (d, J = 7.2 Hz, 1H), 7.32 (m, 10H).

To a solution of (*S*)-benzyl 2-(dimethylamino)-2-oxo-1-phenylethylcarbamate (80.0 g, 256 mmol) in ethanol (1.2 L) was added a slurry of Pd/C (10%, 9.0 g) in ethyl acetate (50 mL). The reaction mixture was shaken in Parr apparatus under hydrogen (40 psi) overnight. The catalyst was removed by filtration through Celite. The filter pad was washed with ethanol (2 × 200 mL), and the combined filtrate was concentrated to give (*S*)-2-amino-*N*,*N*-dimethyl-2-phenylacetamide (40.2 g, 88%) as a white solid. ^{1}H NMR (300 MHz, $CDCl_3$) δ ppm 2.85 (s, 3H), 2.99 (s, 3H), 4.72 (s, 1H), 7.33 (m, 5H).

A flask containing dry THF (2300 mL) under a nitrogen atmosphere was chilled by an ice−water bath. Lithium aluminum hydride (LAH) pellets (59.0 g, 1555 mmol) were added. To this LAH suspension, a solution of (*S*)-2-amino-*N*,*N*-dimethyl-2-phenylacetamide (123.0 g, 691 mmol) in dry THF (800 mL) was slowly added over approximately 1 h. The resulting reaction mixture was heated at reflux for 5 h and then cooled to 10 °C. The cooled reaction mixture was slowly quenched with saturated sodium sulfate solution (380 mL) and stirred overnight. The precipitated solids were filtered off and washed with ethyl acetate (4 × 500 mL). The filtrate was concentrated to a residue that was purified by silica gel chromatography (10% methanol, 5% triethylamine in chloroform) to afford (*S*)-N^1,N^1-dimethyl-2-phenylethane-1,2-diamine (**15a**) (66.7 g, 59%) as a light-yellow liquid. ^{1}H NMR (300 MHz, $CDCl_3$) δ ppm 2.24 (dd, J = 3.6, 12.1 Hz, 1H), 2.29 (s, 6H), 2.47 (dd, J = 10.6, 12.1 Hz, 1H), 4.07 (dd, J = 3.6, 10.4 Hz, 1H), 7.24 (m, 1H), 7.37 (m, 4H).

(*S*)-3-Benzamido-*N*-(2-(dimethylamino)-1-phenylethyl)-6,6-dimethyl-4,6-dihydropyrrolo[3,4-*c*]pyrazole-5(1*H*)-carboxamide (4). A solution of **14** (132.6 mg, 0.339 mmol), (*S*)-N^1,N^1-dimethyl-2-phenylethane-1,2-diamine (**15a**) (87.4 mg, 0.532 mmol), and diisopropylethylamine (0.10 mL, 0.57 mmol) in THF (3.0 mL) was stirred in a 60 °C oilbath for 2 h. The mixture was evaporated to dryness, and the residue was redissolved in methanol (1 mL) and triethylamine (1 mL). After stirring at room temperature for 17 h, the solvents were evaporated and the crude product was purified by silica gel chromatography, eluting with a gradient of 0−20% [EtOH + 5% NH_4OH] in ethyl acetate. The product-containing fractions were concentrated, redissolved in minimal acetonitrile/cyclohexane, and concentrated again to give **4** (83.6 mg, 53%) as a pale-yellow solid. ^{1}H NMR (400 MHz, methanol-d_4) δ ppm 1.69 (s, 3H), 1.75 (s, 3H), 2.35 (s, 6H), 2.47 (dd, J = 12.88, 4.55 Hz, 1H), 2.84 (dd, J = 12.76, 10.48 Hz, 1H), 4.73 (td, J = 11.62, 10.36 Hz, 2H), 5.01 (dd, J = 10.23, 4.42 Hz, 1H), 7.23 (t, J = 7.33 Hz, 1H), 7.33 (dd, J = 7.83, 7.33 Hz, 2H), 7.38 (d, J = 7.33 Hz, 2H), 7.53 (dd, J = 7.83, 7.33 Hz, 2H), 7.61 (t, J = 7.33 Hz, 1H), 7.97 (d, J = 7.33 Hz, 2H). Anal. ($C_{25}H_{30}N_6O_2\cdot0.7H_2O\cdot0.05$cyclohexane) C, H, N. HRMS: [M + H]$^+$ calcd 447.250301, found 447.250246, error −0.12 ppm.

(*S*)-3-Benzamido-*N*-(2-(dimethylamino)-1-phenylethyl)-*N*,6,6-trimethyl-4,6-dihydropyrrolo[3,4-*c*]pyrazole-5(1*H*)-carboxamide (16). By the method used to make **4**, compound **14** (100 mg, 0.256 mmol) and (*S*)-N^1,N^2,N^2-trimethyl-1-phenylethane-1,2-diamine (68 mg, 0.381 mmol) yielded, after reverse-phase preparative HPLC and lyophilization, **16** (15.4 mg, 12%) as an off-white solid. ^{1}H NMR (400 MHz, methanol-d_4) δ ppm 1.76 (d, J = 9.32 Hz, 6H), 2.45 (s, 6H), 2.66 (s, 3H), 3.08 (d, J = 6.04 Hz, 2H), 4.73 (br s, 2H), 5.13 (t, J = 7.30 Hz, 1H), 7.29 (t, J = 7.30 Hz, 1H), 7.38 (t, J = 7.55 Hz, 2H), 7.41−7.46 (m, 2H), 7.51 (t, J = 7.55 Hz, 2H), 7.59 (t, J = 7.18 Hz, 1H), 7.92 (d, J = 7.81 Hz, 2H). Anal. ($C_{26}H_{32}N_6O_2\cdot0.3$HOAc$\cdot0.2H_2O$) C, H, N. HRMS: [M + H]$^+$ calcd 461.265951, found 461.26657, error 1.34 ppm.

***N*-(6,6-Dimethyl-5-(4-methyl-2-phenylpiperazine-1-carbonyl)-1,4,5,6-tetrahydropyrrolo[3,4-*c*]pyrazol-3-yl)benzamide (17).** By the method used to make **4**, compound **14** (130 mg, 0.33 mmol) and racemic 1-methyl-3-phenylpiperazine (145.5 mg, 2.5 equiv) yielded after reverse-phase preparative HPLC and lyophilization, **17** (39.3 mg, 24%) as an off-white solid. ^{1}H NMR (400 MHz, methanol-d_4) δ ppm 1.29 (s, 3H), 1.52 (s, 3H), 2.25−2.34 (m, 4H), 2.45−2.56 (m, 1H), 2.82 (d, J = 10.36 Hz, 1H), 2.87−2.99 (m, 2H), 3.36 (d, J = 12.38 Hz, 1H), 4.11 (dd, J = 10.61, 2.78 Hz, 1H), 4.72−4.77 (m, 1H), 4.85−4.91 (m, 1H), 7.08−7.14 (m, 1H), 7.20 (t, J = 7.58 Hz, 2H), 7.24−7.30 (m, 2H), 7.42−7.48 (m, 2H), 7.50−7.56 (m, 1H), 7.89 (d, J = 7.33 Hz, 2H). Anal. ($C_{26}H_{30}N_6O_2\cdot0.5$HOAc$\cdot0.5H_2O$) C, H, N. HRMS: [M + H]$^+$ calcd 459.250301, found 459.250487, error 0.4 ppm.

(*S*)-2-(Dimethylamino)-1-phenylethanol (15b). Formaldehyde (46.8 mL, 37 wt % in water) was added slowly to a solution of (*S*)-(+)-2-amino-1-phenyl-ethanol (11.70 g, 85.3 mmol) in 88% formic acid (46.8 mL) at room temperature. The solution was stirred in a 95 °C oil bath for 19 h. After cooling to room temperature, concd HCl was added to adjust the solution to pH = 2. After extracting with ether (75 mL), the remaining aqueous layer was cooled in an ice bath while 50% sodium hydroxide was added to raise the pH to 10. The resulting basic aqueous solution was extracted with dichloromethane (2 × 200 mL). The combined organic extracts were dried over magnesium sulfate, filtered, and concentrated. The crude product was purified by silica gel chromatography, eluting with a gradient of 5−20% [ethanol + 5%NH_4OH] in ethyl acetate, to give (*S*)-2-(dimethylamino)-1-phenylethanol (**15b**) as a light-yellow oil (12.13 g, 86%). ^{1}H NMR (400 MHz, DMSO-d_6) δ ppm 2.19 (s, 6H), 2.30 (dd, J = 12.38, 4.80 Hz, 1H), 2.42 (dd, J = 12.38, 8.08 Hz, 1H), 4.63 (dd, J = 7.96, 4.93 Hz, 1H), 4.97 (br s, 1H), 7.18−7.24 (m, 1H), 7.26−7.35 (m, 4H). Anal. ($C_{10}H_{15}NO\cdot0.13H_2O$) C, H, N.

(*S*)-2-(Dimethylamino)-1-phenylethyl 3-benzamido-6,6-dimethyl-4,6-dihydropyrrolo[3,4-*c*]pyrazole-5(1*H*)-carboxylate (18). A solution of potassium carbonate (861 mg, 6.23 mmol), intermediate **14** (1.218 g, 3.12 mmol), and alcohol **15b** (772 mg, 4.67 mmol) in 1,2-dimethoxyethane (DME, 31 mL) was stirred in an 80 °C oil bath for 7.5 h. After cooling to room temperature, the solvent was evaporated and the residue partitioned between ethyl acetate (25 mL) and deionized water (20 mL). The aqueous layer was back-extracted with ethyl acetate (2 × 15 mL) and the combined organic extracts dried over magnesium sulfate, filtered, and concentrated to dryness. The residue was dissolved in methanol (10 mL) and triethylamine (10 mL), stirred at room temperature for 19 h, and again concentrated to dryness. The crude product was purified by silica gel chromatography, eluting with a gradient of 5−20% [ethanol + 5% NH_4OH] in ethyl acetate, affording compound **18** (561.1 mg, 39%) as a white foam. ^{1}H NMR (400 MHz, methanol-d_4) δ ppm 1.62 (s, 3H), 1.73 (s, 3H), 2.39 (s, 6H), 2.56 (dd, J = 13.64, 3.28 Hz, 1H), 2.98 (dd, J = 13.39, 9.60 Hz, 1H), 5.91 (dd, J = 9.47, 3.16 Hz, 1H), 7.27−7.46 (m, 5H), 7.48−7.65 (m, 3H), 7.91−8.00 (m, 2H), (some peaks may be obscured by solvent signals). Anal. ($C_{25}H_{29}N_5O_3\cdot0.03$EtOAc$\cdot0.35H_2O$) C, H, N. HRMS: [M + H]$^+$ calcd 448.2343; found 448.2341; error −0.39 ppm.

(*S*)-2-(Dimethylamino)-1-phenylethyl-3-(4-fluorobenzamido)-6,6-dimethyl-4,6-dihydropyrrolo[3,4-*c*]pyrazole-5(1*H*)-carboxylate (19). By the method used to make compound **18**, intermediate **14a** (5.46 g, 13.36 mmol) and alcohol **15b** (3.31 g, 20.03 mmol) gave, after purification by silica gel chromatography and recrystallization from dichloromethane/cyclohexane, compound **19** (2.76 g, 44%) as a white solid. ^{1}H NMR (400 MHz, methanol-d_4) δ ppm 1.62 (s, 3H), 1.72 (s, 3H), 2.38 (s, 6H), 2.56 (dd, J = 13.52, 3.16 Hz, 1H), 2.98 (dd, J = 13.64, 9.60 Hz, 1H), 4.58 (br s, 1H), 4.79 (br s, 1H), 5.91 (dd, J = 9.47, 3.16 Hz, 1H), 7.20−7.33 (m, 3H), 7.33−7.47

dx.doi.org/10.1021/jm300204j | J. Med. Chem. XXXX, XXX, XXX−XXX

(m, 4H), 8.04 (dd, J = 8.59, 5.31 Hz, 2H). Anal. ($C_{25}H_{28}FN_5O_3$·0.35H_2O) C, H, N, F. HRMS: $[M + H]^+$ calcd 466.22489; found 466.22468; error −0.46 ppm.

(*S*)-*N*-(2-(Dimethylamino)-1-phenylethyl)-3-(2-fluorobenzamido)-6,6-dimethyl-4,6-dihydropyrrolo[3,4-*c*]pyrazole-5(1*H*)-carboxamide (20). By the method used to make compound **4**, compound **32** (120 mg, 0.29 mmol) and (*S*)-N^1,N^1-dimethyl-2-phenylethane-1,2-diamine (**15a**) (71 mg, 0.43 mmol) yielded, after reverse-phase prep HPLC and lyophilization, **20** (50 mg, 36%) as a white solid. ^{1}H NMR (400 MHz, methanol-d_4) δ ppm 1.68 (s, 3H), 1.75 (s, 3H), 2.45 (s, 6H), 2.62 (dd, J = 12.72, 4.41 Hz, 1H), 2.91−3.03 (m, 1H), 4.67−4.82 (m, 2H), 5.07 (dd, J = 10.70, 4.41 Hz, 1H), 7.21−7.43 (m, 7H), 7.52−7.66 (m, 1H), 7.78−7.89 (m, 1H). Anal. ($C_{25}H_{29}N_6O_2F$·0.2HOAc·0.4H_2O) C, H, N. HRMS: $[M + H]^+$ calcd 465.240879, found 465.241357, error 1.03 ppm.

(*S*)-2-(Dimethylamino)-1-phenylethyl 3-(2,4-Difluorobenzamido)-6,6-dimethyl-4,6-dihydropyrrolo[3,4-*c*]pyrazole-5(1*H*)-carboxylate (21). By the method used to make compound **18**, compound **33** (240 mg, 0.56 mmol) and alcohol **15b** (139 mg, 0.84 mmol) yielded, after reverse-phase prep HPLC and lyophilization, **21** as a white solid (54.9 mg, 19%). ^{1}H NMR (400 MHz, methanol-d_4) δ ppm 1.63 (s, 3H), 1.74 (s, 3H), 2.57 (s, 6H), 2.81 (dd, J = 13.39, 3.03 Hz, 1H), 3.15−3.26 (m, 1H), 4.75−4.85 (m, 2H), 5.99 (dd, J = 9.85, 3.03 Hz, 1H), 7.11−7.21 (m, 2H), 7.33−7.45 (m, 5H), 7.84−7.96 (m, 1H). Anal. ($C_{25}H_{27}N_5O_3F_2$·0.4HOAc) C, H, N. HRMS: $[M + H]^+$ calcd 484.215473, found 484.214847, error −1.29 ppm.

(*S*)-2-(Dimethylamino)-1-phenylethyl 6,6-Dimethyl-3-(picolinamido)-4,6-dihydropyrrolo[3,4-*c*]pyrazole-5(1*H*)-carboxylate (22). By the method used to make compound **18**, compound **34** (120 mg, 0.306 mmol) and alcohol **15b** (76 mg, 0.46 mmol) yielded, after reverse-phase prep HPLC and lyophilization, **22** as a white solid (54 mg, 37%). ^{1}H NMR (400 MHz, MeOD) δ ppm 1.61 (s, 3H), 1.72 (s, 3H), 2.54 (s, 6H), 2.77 (d, J = 13.60 Hz, 1H), 3.08−3.24 (m, 1H), 4.56−4.79 (m, 1H), 4.91−5.03 (m, 1H), 5.90−6.05 (m, 1H), 7.29−7.36 (m, 1H), 7.36−7.49 (m, 4H), 7.58−7.69 (m, 1H), 7.99−8.09 (m, 1H), 8.21 (d, J = 7.81 Hz, 1H), 8.71 (d, J = 4.78 Hz, 1H). Anal. ($C_{24}H_{28}N_6O_3$·0.4HOAc·0.2H_2O) C, H, N. HRMS: $[M + H]^+$ calcd 449.229565, found 449.229005, error −1.25 ppm.

(*S*)-2-(Dimethylamino)-1-phenylethyl 6,6-Dimethyl-3-pivalamido-4,6-dihydropyrrolo[3,4-*c*]pyrazole-5(1*H*)-carboxylate (23). By the method used to make compound **18**, compound **35** (250.9 mg, 0.677 mmol), and alcohol **15b** (237.0 mg, 1.434 mmol) yielded, after silica gel chromatography and trituration from cyclohexane, **23** (109.3 mg, 35%) as a white powder. ^{1}H NMR (400 MHz, methanol-d_4) δ ppm 1.30 (s, 9H), 1.58 (s, 3H), 1.69 (s, 3H), 2.38 (s, 6H), 2.55 (dd, J = 13.52, 3.16 Hz, 1H), 2.97 (dd, J = 13.39, 9.60 Hz, 1H), 4.63−4.81 (m, 2H), 5.90 (dd, J = 9.35, 3.03 Hz, 1H), 7.26−7.45 (m, 5H). Anal. ($C_{23}H_{33}N_5O_3$·0.7H_2O·0.3cyclohexane) C, H, N. HRMS: $[M + H]^+$ calcd 428.265616, found 428.265349, error −0.62 ppm.

(*S*)-2-(Dimethylamino)-1-phenylethyl 6,6-Dimethyl-3-(tetrahydrofuran-2-carboxamido)-4,6-dihydropyrrolo[3,4-*c*]-pyrazole-5(1*H*)-carboxylate (24). By the method used to make compound **18**, compound **36** (225.0 mg, 0.585 mmol) and alcohol **15b** (145 mg, 0.877 mmol) yielded, after silica gel chromatography and trituration from cyclohexane, **24** (121.5 mg, 45%, mixture of diastereomers) as a white powder. ^{1}H NMR (400 MHz, methanol-d_4) δ ppm 1.59 (s, 3H), 1.69 (s, 3H), 1.91−2.15 (m, 3H), 2.38 (s, 6H), 2.56 (dd, J = 13.52, 3.16 Hz, 1H), 2.96 (dd, J = 13.39, 9.60 Hz, 1H), 3.87−3.98 (m, 1H), 4.02−4.12 (m, 1H), 4.46 (dd, J = 8.08, 6.32 Hz, 2H), 4.62−4.80 (m, 2H), 5.89 (dd, J = 9.35, 3.03 Hz, 1H), 7.26−7.46 (m, 5H). Anal. ($C_{23}H_{31}N_5O_4$·0.15cyclohexane·0.6H_2O) C, H, N. HRMS: $[M + H]^+$ calcd 442.2449; found 442.2446, error −0.62 ppm.

(*S*)-2-(Dimethylamino)-1-phenylethyl 6,6-Dimethyl-3-(tetrahydro-2*H*-pyran-2-carboxamido)-4,6-dihydropyrrolo[3,4-*c*]-pyrazole-5(1*H*)-carboxylate (25). By the method used to make compound **18**, compound **37** (229.8 mg, 0.576 mmol) and alcohol **15b** (143 mg, 0.864 mmol) yielded, after silica gel chromatography and trituration from cyclohexane, **25** (162.9 mg, 60%, mixture of diastereomers) as an off-white foam. ^{1}H NMR (400 MHz, methanol-d_4) δ ppm 1.48−1.67 (m, 6H), 1.69 (s, 3H), 1.89−2.11 (m, 2H), 2.37 (s, 6H), 2.55 (dd, J = 13.64, 3.03 Hz, 1H), 2.95 (dd, J = 13.52, 9.73 Hz, 1H), 3.53−3.65 (m, 1H), 3.90−4.01 (m, 1H), 4.07−4.17 (m, 1H), 4.50 (br s, 1H), 4.66−4.82 (m, 2H), 5.89 (dd, J = 9.35, 1.52 Hz, 1H), 7.26−7.45 (m, 5H). Anal. ($C_{24}H_{33}N_5O_4$·0.1cyclohexane·0.5H_2O) C, H, N. HRMS: $[M + H]^+$ calcd 456.2606; found 456.2597, error −1.92 ppm.

5-*tert*-Butyl 1-Ethyl 6,6-Dimethyl-3-(3,3,3-trifluoro-2,2-dimethylpropanamido)pyrrolo[3,4-*c*]pyrazole-1,5(4*H*,6*H*)-dicarboxylate (38). DMF (0.8 mL) was added to a cooled (0 °C) solution of 3,3,3-trifluoro-2,2-dimethylpropanoic acid (3.0 g, 20 mmol) in dichloromethane (60 mL), and then a solution of freshly distilled oxalyl chloride (2.8 g, 22 mmol) in dichloromethane (15 mL) was added dropwise, causing slight gas evolution. The mixture was stirred for 6 h, allowing it to gradually warm to room temperature and then recooled to 0 °C. 5-*tert*-Butyl 1-ethyl 3-amino-6,6-dimethylpyrrolo[3,4-*c*]pyrazole-1,5(4*H*,6*H*)-dicarboxylate (**11−2**) (2.7 g, 8.3 mmol) was added, followed by diisopropylethylamine (11.4 mL). The mixture was stirred for 15 h, allowing it to gradually warm to room temperature. The solution was cooled again to 0 °C and treated with 5% aqueous HCl (25 mL). The layers were separated, and the aqueous layer extracted with dichloromethane (25 mL). The combined organic layers were dried over sodium sulfate, filtered, and concentrated. The crude product was purified on a silica plug, eluting with 30% ethyl acetate in heptane, affording **38** (2.48 g, 64%) as a white solid. ^{1}H NMR (400 MHz, chloroform-d) δ ppm 1.46 (d, J = 6.80 Hz, 3H), 1.48−1.60 (m, 15H), 1.78 (d, J = 6.04 Hz, 3H), 1.80 (s, 3H), 4.60 (q, J = 7.22 Hz, 2H), 4.84 (s, 1H), 4.92 (d, J = 53.38 Hz, 1H), 10.83 (br s, 1H).

Ethyl 6,6-Dimethyl-3-(3,3,3-trifluoro-2,2-dimethylpropanamido)-5,6-dihydropyrrolo[3,4-*c*]pyrazole-1(4*H*)-carboxylate (39). A solution of **38** (3.2 g, 6.9 mmol) in ethyl acetate (60 mL) was treated with 4.0 M HCl solution in dioxane (40 mL) for 14 h at room temperature. The solvents were evaporated, and the residual solid triturated with ether to give the monohydrochloride salt of **39** (2.2 g, 80%) as a white solid. ^{1}H NMR (400 MHz, DMSO-d_6) ppm 1.36 (t, J = 7.18 Hz, 3H), 1.49 (s, 6H), 1.65 (s, 6H), 4.46 (q, J = 7.13 Hz, 2H), 4.51 (s, 2H), 10.16 (br s, 2H), 10.59 (s, 1H). Anal. ($C_{15}H_{21}F_3N_4O_3$·1.0HCl) C, H, N, F, Cl.

Ethyl 5-(Chlorocarbonyl)-6,6-dimethyl-3-(3,3,3-trifluoro-2,2-dimethylpropanamido)-5,6-dihydropyrrolo[3,4-*c*]pyrazole-1(4*H*)-carboxylate (40). A solution of monohydrochloride salt **39** (1.2 g, 3.0 mmol) in dichloromethane (40 mL) was cooled to −78 °C. Diisopropylethylethylamine (1.9 mL) was added, followed by a solution of triphosgene (630 mg, 2.1 mmol) in dichloromethane (10 mL). The mixture was stirred for 20 min and then quenched while cold with saturated aqueous sodium bicarbonate solution (25 mL). The resulting biphasic mixture was allowed to warm to room temperature, the layers were separated, and the aqueous layer was extracted with dichloromethane (25 mL). The combined organic extracts were dried over sodium sulfate, filtered, and concentrated to a white solid. The crude product was purified by passing through a silica plug, eluting with 20% ethyl acetate in heptane, to give **40** (1.13 g, 88%) as a white solid. ^{1}H NMR (400 MHz, chloroform-d) δ ppm 1.45−1.56 (m, 9H), 1.78 (s, 6H), 4.60 (q, J = 7.05 Hz, 2H), 4.98 (s, 2H), 10.83 (br s, 1H).

A similar three-step procedure was used to make the following two compounds

Ethyl 5-(Chlorocarbonyl)-6,6-dimethyl-3-(1-(trifluoromethyl)cyclopropanecarboxamido)-5,6-dihydropyrrolo[3,4-*c*]pyrazole-1(4*H*)-carboxylate (41). ^{1}H NMR (400 MHz, chloroform-d) δ ppm 1.39−1.44 (m, 2H), 1.47−1.54 (m, 3H), 1.56 (br s, 2H), 1.76−1.81 (m, 6H), 4.61 (q, J = 7.13 Hz, 2H), 4.77 (s, 1H), 4.92 (s, 1H), 11.06 (br s, 1H).

Ethyl 5-(Chlorocarbonyl)-6,6-dimethyl-3-(1-(trifluoromethyl)cyclobutanecarboxamido)-5,6-dihydropyrrolo[3,4-*c*]pyrazole-1(4*H*)-carboxylate (42). ^{1}H NMR (400 MHz, chloroform-d) δ ppm 1.48 (t, J = 7.05 Hz, 3H), 1.78 (s, 6H), 1.97−2.21 (m, 2H), 2.51−2.72 (m, 4H), 4.57 (q, J = 7.22 Hz, 2H), 5.00 (s, 2H), 10.57 (br s, 1H).

(*S*)-2-(Dimethylamino)-1-phenylethyl 6,6-Dimethyl-3-(3,3,3-trifluoro-2,2-dimethylpropanamido)-4,6-dihydropyrrolo[3,4-

dx.doi.org/10.1021/jm300204j | *J. Med. Chem.* XXXX, XXX, XXX−XXX

c]pyrazole-5(1*H*)-carboxylate (26). By the method used to make compound **18**, compound **40** (7.69 g, 18.10 mmol), and alcohol **15b** (6.00 g, 36 mmol) yielded, after reverse-phase preparative HPLC, **26** (5.10 g, 44%) as a white solid. ^{1}H NMR (700 MHz, DMSO-d_6) δ ppm 1.47 (s, 3H), 1.48 (s, 3H), 1.51 (s, 3H), 1.63 (s, 3H), 2.90 (br s, 6H), 3.40−3.51 (m, 1H), 3.77 (t, J = 12.16 Hz, 1H), 4.58 (d, J = 13.27 Hz, 1H), 4.85 (d, J = 13.27 Hz, 1H), 6.15 (d, J = 11.06 Hz, 1H), 7.35−7.53 (m, 5H), 9.62 (br s, 1H), 10.44 (s, 1H). Anal. ($C_{23}H_{30}F_3N_5O_3$·1.36TFA·0.28H_2O) C, H, N.

(*S*)-2-(Dimethylamino)-1-phenylethyl 6,6-Dimethyl-3-(1-(trifluoromethyl)cyclopropanecarboxamido)-4,6-dihydropyrrolo[3,4-*c*]pyrazole-5(1*H*)-carboxylate (27). By the method used to make compound **18**, compound **41** (6.69 g, 15.8 mmol) and alcohol **15b** 5.23 g, 31.6 mmol) yielded, after reverse-phase preparative HPLC, **27** (5.05 g, 63%) as a white solid. ^{1}H NMR (400 MHz, methanol-d_4) δ ppm 1.32−1.49 (m, 5H), 1.58 (s, 3H), 1.70 (s, 3H), 2.54 (s, 6H), 2.77 (d, J = 13.85 Hz, 1H), 3.14−3.27 (m, 1H), 4.68 (d, J = 13.09 Hz, 1H), 4.79 (d, J = 13.35 Hz, 1H), 5.96 (dd, J = 9.95, 2.64 Hz, 1H), 7.28−7.46 (m, 6H). Anal. ($C_{23}H_{28}F_3N_5O_3$·0.3HOAc·0.1H_2O) C, H, N. HRMS: $[M + H]^+$ calcd 480.221701, found 480.222644, error 1.96 ppm.

(*S*)-2-(Dimethylamino)-1-phenylethyl 6,6-Dimethyl-3-(1-(trifluoromethyl)cyclobutanecarboxamido)-4,6-dihydropyrrolo[3,4-*c*]pyrazole-5(1*H*)-carboxylate (28). By the method used to make compound **18**, compound **42** (1.00 g, 2.29 mmol) and alcohol **15b** (567 mg, 3.43 mmol) yielded, after reverse phase preparative HPLC, **28** (525 mg, 45%) as a white solid. ^{1}H NMR (400 MHz, methanol-d_4) δ ppm 1.60 (s, 3H), 1.71 (s, 3H), 1.95−2.04 (m, 1H), 2.04−2.16 (m, 1H), 2.50 (s, 6H), 2.51−2.62 (m, 2H), 2.64−2.77 (m, 3H), 3.06−3.17 (m, 1H), 4.70 (d, J = 13.35 Hz, 1H), 4.81 (d, J = 13.35 Hz, 1H), 5.94 (dd, J = 9.82, 3.02 Hz, 1H), 7.29−7.46 (m, 5H). Anal. ($C_{23}H_{28}F_3N_5O_3$·0.2HOAc·0.2H_2O) C, H, N. HRMS: $[M + H]^+$ calcd494.237351, found 494.237453, error 0.21 ppm.

Evaluation of Biological Activities. Experimental procedures for measuring enzymatic activity (K_i), biomarker cellular activity (pGEF-H1 EC_{50}), and in vivo tumor growth inhibition (TGI) have been described.[13]

AUTHOR INFORMATION

Corresponding Author

*For C.G.: phone, (760) 542-8021; E-mail: alexguo01@gmail.com. For I.M.: phone, (858) 622-6061; E-mail: indrawan.mcalpine@pfizer.com.

Notes

The authors declare no competing financial interest.

ABBREVIATIONS USED

ADME absorption, distribution, metabolism and elimination; bid twice a day dosing; DMSO dimethyl sulfoxide; ER extraction ratio; Fpo oral bioavailability; GTPase guanosine triphosphatase; GEF guanine nucleotide exchange factors; HTS high-throughput screening; HLM human liver microsomes; LE ligand efficiency based on number of heavy atoms; LipE ligand efficiency based on lipophilicity; PAK P21-Activated Kinase; PK pharmacokinetic; PSA prostate specific antigen; SAR structure−activity relationship; SBDD structural-based drug design; TGI tumor growth inhibition

REFERENCES

(1) Qiu, R. G.; Chen, J.; McCormick, F.; Symons, M. A role for Rho in Ras transformation. *Proc. Natl. Acad. Sci. U.S.A.* **1995**, *92*, 11781.

(2) Zohn, I. M.; Campbell, S. L.; Khosravi-Far, R.; Rossman, K. L.; Der, C. J. Rho family proteins and Ras transformation: the RHOad less traveled gets congested. *Oncogene* **1998**, *17*, 1415.

(3) Jaffe, A. B.; Hall, A. Rho GTPases: Biochemistry and Biology. *Annu. Rev. Cell Dev. Biol.* **2005**, *21*, 247.

(4) Ellenbroek, S. I.; Collard, J. G. Rho GTPases: functions and association with cancer. *Clin. Exp. Metastasis* **2007**, *24*, 657.

(5) Vega, F. M.; Ridley, A. J. Rho GTPases in cancer cell biology. *FEBS Lett.* **2008**, *582*, 2093.

(6) Arias-Romero, L. E.; Chernoff, J. A tale of two Paks. *Biol. Cell* **2008**, *100*, 97.

(7) Dummler, B.; Ohshiro, K.; Kumar, R.; Field, J. Pak protein kinases and their role in cancer. *Cancer Metastasis Rev.* **2009**, *28*, 51.

(8) Eswaran, J.; Soundararajan, M.; Kumar, R.; Knapp, S. UnPAKing the class differences among p21-activated kinases. *Trends Biochem. Sci.* **2008**, *33*, 394.

(9) Molli, P. R.; Li, D. Q.; Murray, B. W.; Rayala, S. K.; Kumar, R. PAK signaling in oncogenesis. *Oncogene* **2009**, *28*, 2545.

(10) Birkenfeld, J.; Nalbant, P.; Yoon, S.-H.; Bokoch, G. M. Cellular functions of GEF-H1, a microtubule-regulated Rho-GEF: Is altered GEF-H1 activity a crucial determinant of disease pathogenesis? *Trends Cell Biol.* **2008**, *18* (6), 210−219.

(11) Vadlamudi, R. K.; Adam, L.; Wang, R. A.; Mandal, M.; Nguyen, D.; Sahin, A.; Chernoff, J.; Hung, M. C.; Kumar, R. Regulatable Expression of p21-activated Kinase-1 Promotes Anchorage-Independent Growth and Abnormal Organization of Mitotic Spindles in Human Epithelial Breast Cancer Cells. *J. Biol. Chem.* **2000**, *275*, 36238.

(12) Qu, J.; Cammarano, M. S.; Shi, Q.; Ha, K. C.; de Lanerolle, P.; Minden, A. Activated PAK4 Regulates Cell Adhesion and Anchorage-Independent Growth. *Mol. Cell. Biol.* **2001**, *21*, 3523.

(13) Callow, M. G.; Clairvoyant, F.; Zhu, S.; Schryver, B.; Whyte, D. B.; Bischoff, J. R.; Jallal, B.; Smeal, T. Requirement for PAK4 in the Anchorage-Independent Growth of Human Cancer Cell Lines. *J. Biol. Chem.* **2002**, *277*, 550.

(14) Murray, B. W.; Guo, C.; Piraino, J.; Westwick, J. K.; Zhang, C.; Lamerdin, J.; Dagostino, E.; Knighton, D.; Loi, C. M.; Zager, M.; Kraynov, E.; Popoff, I.; Christensen, J. G.; Martinez, R.; Kephart, S. E.; Marakovits, J.; Karlicek, S.; Bergqvist, S.; Smeal, T. Small-molecule p21-activated kinase inhibitor PF-3758309 is a potent inhibitor of oncogenic signaling and tumor growth*Proc. Natl. Acad. Sci. U.S.A. 107*, 9446−9451.

(15) Ong, C. C.; Jubb, A. M.; Haverty, P. M.; Zhou, W.; Tran, V.; Truong, T.; Turley, H.; O'Brien, T.; Vucic, D.; Harris, A. L.; Belvin, M.; Friedman, L. S.; Blackwood, E. M.; Koeppen, H.; Hoeflich, K. P. Targeting p21-activated kinase 1 (PAK1) to induce apoptosis of tumor cells *Proc. Natl. Acad. Sci. U.S.A.* **2011***108*, 7177−7182.

(16) Kuntz, I. D.; Chen, K.; Sharp, K. A.; Kollman, P. A. The maximal affinity of ligands. *Proc. Natl. Acad. Sci. U.S.A.* **1999**, *96*, 9997−10002.

(17) All log *D* values cited herein are experimental data following Analiza's octanol/buffer partitioning method. Link: *Analiza*; Analiza, Inc.: Cleveland, OH; http://www.analiza.com/adme/adme-services.html.

(18) Brasca, M. G.; Amici, R.; Fancelli, D.; Nesi, M.; Orsini, P.; Orzi, F.; Roussel, P.; Vulpetti, A.; Pevarello, P. Substituted Pyrrolo-Pyrazole Derivatives As Kinase Inhibitors. PCT Int. Appl. WO 2004056827 A2 20040708, 2004.

(19) Both regioisomers can be used for preparing the target molecules reported herein. We usually separated the two (**11−1** and **11−2**) and used them separately for ease of analysis.

(20) Press, B.; Di Grandi, D. Permeability for Intestinal Absorption: Caco-2 and Related Issues. *Curr. Drug Metab.* **2008**, *9*, 893 and references cited therein..

(21) Compounds **24** and **25** were mixtures of diasteromers. See Experimental Section.